Since January 2020 Elsevier has created a COVID-19 resource centre with free information in English and Mandarin on the novel coronavirus COVID-19. The COVID-19 resource centre is hosted on Elsevier Connect, the company's public news and information website.

Article

Cell Reports

Profiling CD8$^+$ T cell epitopes of COVID-19 convalescents reveals reduced cellular immune responses to SARS-CoV-2 variants

Graphical abstract

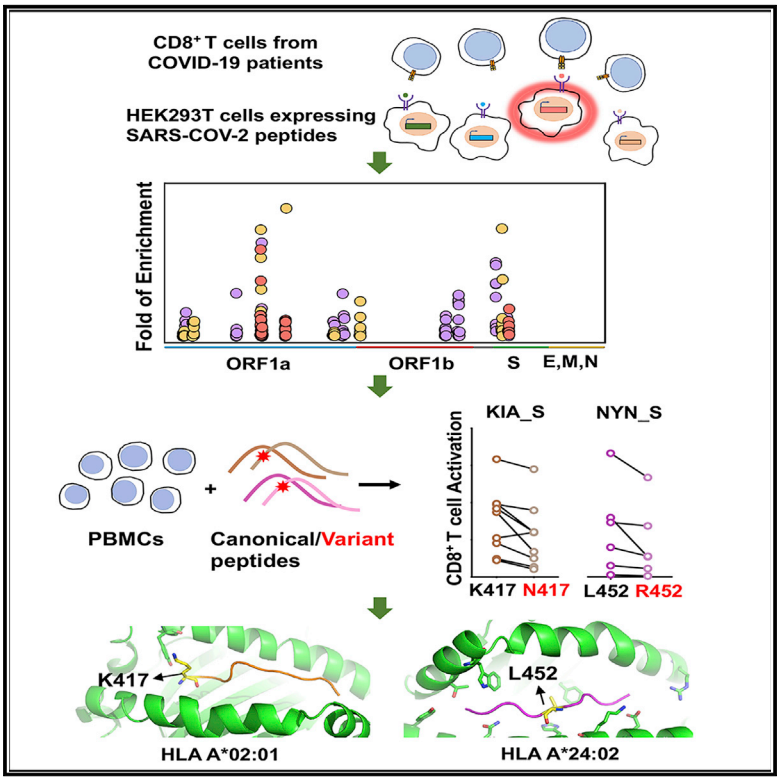

Highlights

- Systematic analysis of CD8$^+$ T cell epitopes of SARS-CoV-2 in convalescent samples
- CD8$^+$ T cell epitopes highly conserved among human coronaviruses are identified
- SARS-CoV-2 variants harbor multiple mutations that reduce cellular immune responses
- K417 and L452 of SARS-CoV-2 spike protein are critical in mediating recognition by HLA

Authors

Hang Zhang, Shasha Deng, Liting Ren, Peiyi Zheng, Xiaowen Hu, Tengchuan Jin, Xu Tan

Correspondence

jint@ustc.edu.cn (T.J.), xutan@tsinghua.edu.cn (X.T.)

In brief

Zhang et al. report a systematic analysis of SARS-CoV-2 peptide epitopes in COVID-19 convalescent samples and reveal highly conserved epitopes as well as mutations in SARS-CoV-2 variants that reduce cellular immune responses. In particular, two mutations in the Delta and Delta plus variants are critical in mediating immune recognition.

Zhang et al., 2021, Cell Reports *36*, 109708
September 14, 2021
https://doi.org/10.1016/j.celrep.2021.109708

CellPress

Cell Reports

CellPress
OPEN ACCESS

Article

Profiling CD8$^+$ T cell epitopes of COVID-19 convalescents reveals reduced cellular immune responses to SARS-CoV-2 variants

Hang Zhang,[1,2,6] Shasha Deng,[3,6] Liting Ren,[1] Peiyi Zheng,[3] Xiaowen Hu,[4] Tengchuan Jin,[3,4,5,*] and Xu Tan[1,2,7,*]

[1]Beijing Advanced Innovation Center for Structural Biology, Beijing Frontier Research Center for Biological Structure, MOE Key Laboratory of Bioorganic Phosphorus Chemistry & Chemical Biology, School of Pharmaceutical Sciences, Tsinghua University, Beijing 100084, China
[2]Tsinghua-Peking Center for Life Sciences, Beijing 100084, China
[3]Hefei National Laboratory for Physical Sciences at Microscale, CAS Key Laboratory of Innate Immunity and Chronic Disease, School of Basic Medical Sciences, Division of Life Sciences and Medicine, University of Science and Technology of China, Hefei 230027, China
[4]Department of Pulmonary and Critical Care Medicine, The First Affiliated Hospital of USTC, Division of Life Sciences and Medicine, University of Science and Technology of China, Hefei, Anhui 230001, China
[5]CAS Center for Excellence in Molecular Cell Science, Chinese Academy of Sciences, Shanghai 200031, China
[6]These authors contributed equally
[7]Lead contact
*Correspondence: jint@ustc.edu.cn (T.J.), xutan@tsinghua.edu.cn (X.T.)
https://doi.org/10.1016/j.celrep.2021.109708

SUMMARY

Cellular immunity is important in determining the disease severity of COVID-19 patients. However, current understanding of SARS-CoV-2 epitopes mediating cellular immunity is limited. Here we apply T-Scan, a recently developed method, to identify CD8$^+$ T cell epitopes from COVID-19 patients of four major HLA-A alleles. Several identified epitopes are conserved across human coronaviruses, which might mediate pre-existing cellular immunity to SARS-CoV-2. In addition, we identify and validate four epitopes that were mutated in the newly circulating variants, including the Delta variant. The mutations significantly reduce T cell responses to the epitope peptides in convalescent and vaccinated samples. We further determine the crystal structure of HLA-A*02:01/HLA-A*24:02 in complex with the epitope KIA_S/NYN_S, respectively, which reveals the importance of K417 and L452 of the spike protein for binding to HLA. Our data suggest that evading cellular immunity might contribute to the increased transmissibility and disease severity associated with the new SARS-CoV-2 variants.

INTRODUCTION

The COVID-19 epidemic has caused the infection of over 200 million people and deaths of over 4 million people worldwide as of August 2021 (https://www.who.int/emergencies/diseases/novel-coronavirus-2019). Although the global efforts of vaccination promise to greatly reduce the infection and mortality caused by SARS-CoV-2, recently emerging variants that are more transmissible might be less responsive to currently available vaccines (Campbell et al., 2021; Collier et al., 2021; Garcia-Beltran et al., 2021; Gómez et al., 2021; Wang et al., 2021a). Therefore, these variants present serious challenges to the prevention of infection and control of the epidemic (Calistri et al., 2021; Challen et al., 2021). It is imperative to understand the mechanism underlying the recent explosive transmission of the emerging variants. Recently, a series of studies have revealed that these variants are more resistant to previously isolated neutralizing antibodies or convalescent sera from infection by the canonical SARS-CoV-2 variant (Cele et al., 2021; Chen et al., 2021; Collier et al., 2021; Halfmann et al., 2020; Hoffmann et al., 2021; Plante et al., 2021; Volz et al., 2021; Wang et al., 2021b). These studies sounded an alert to the efficacy of currently used vaccines and antibodies for the variants. However, these findings do not directly explain why these variants rapidly become dominating variants in certain countries and spread globally, as most infected people are first-time infected and unvaccinated. There are also mixed findings regarding the infectivity of these variants, which might not be the main reason underlying their transmissibility (Hou et al., 2020; Neches et al., 2021; Ozono et al., 2021; Plante et al., 2021; Volz et al., 2021; Yurkovetskiy et al., 2020).

In a number of studies, cellular immunity has been shown to strongly correlate with disease outcome (Le Bert et al., 2021; Sattler et al., 2020; Sekine et al., 2020; Tan et al., 2021; Weiskopf et al., 2020), which indicates the importance of understanding the difference in cellular immunity for the various variants. Previous studies have used limited numbers of synthetic peptides to identify epitopes that activate CD8$^+$ T cells from COVID-19 patients or convalescents (Grifoni et al., 2020; Kared et al., 2021; Le Bert et al., 2020; Peng et al., 2020; Schulien et al., 2021; Shomuradova et al., 2020; Weiskopf et al., 2020). These studies have revealed a number of CD8$^+$ T cell epitopes that are conserved between SARS-CoV-2 and other human coronaviruses that

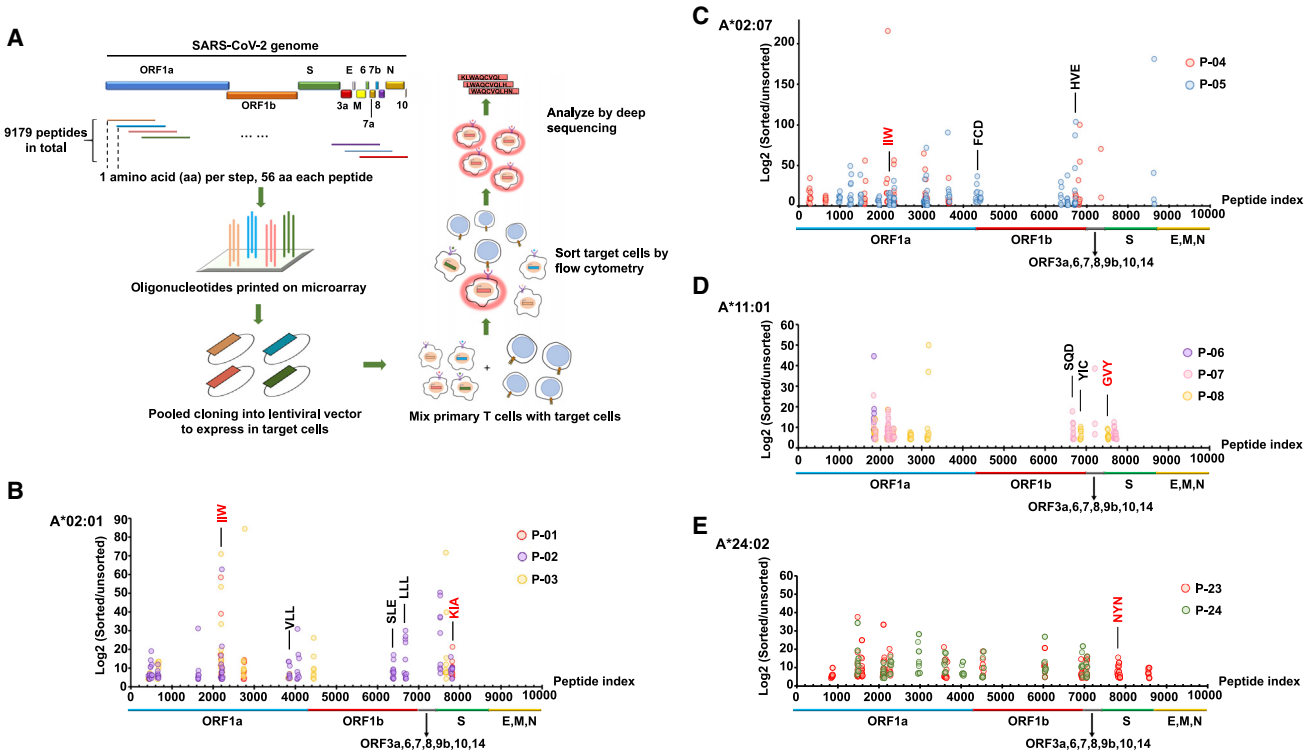

Figure 1. Profiling of CD8$^+$ T cell epitopes of COVID-19 convalescent patients through the T-Scan approach

(A) Design of the genome-wide SARS-CoV-2 antigen library and the overview of the T-Scan epitope identification screening. T cells from COVID-19 convalescent patients recognize target epitopes and activate the T-scan reporter.

(B–E) T-Scan screen data for ten COVID-19 convalescents (P-01 to P-08, P23, and P24), three with the HLA-A*02:01 genotype, two with the HLA-A*02:07 genotype, three with the HLA-A*11:01 genotype, and two with the HLA-A*24:02 genotype. Each circle represents a 56-amino-acid (aa) peptide tile of the SARS-CoV-2 open reading frame (ORF). The x axis shows the peptide index of our designed genome-wide SARS-CoV-2 antigen library, with the y axis indicating the fold enrichment ratio of each peptide in sorted target cells compared with the corresponding unsorted EDC library.

cause the common cold, which provided evidence for pre-existing immunity in people previously infected by common-cold-causing coronaviruses. One study used a systematic method named T-Scan to profile epitopes but identified very few epitopes conserved across human coronaviruses (Ferretti et al., 2020). Also surprisingly, few epitopes in the spike protein of SARS-CoV-2 were identified in this study compared with other studies (Ferretti et al., 2020; Le Bert et al., 2020; Shomuradova et al., 2020). T-Scan utilizes a reporter-cell-based epitope-expressing library to incubate with human CD8$^+$ T cells to identify epitopes that can activate CD8$^+$ T cells in an unbiased fashion (Kula et al., 2019). The reporter cells (epitope discovery cells; EDCs) overexpress an HLA subtype and a peptide from the proteome of the pathogens of interest. In addition, the EDCs also overexpress a modified infrared fluorescence protein (IFP) containing a GzB cleavage sequence with fluorescence appearance only after being cleaved by GzB. When the EDCs presenting the cognate epitopes activate CD8$^+$ T cells, which secrete GzB into the cognate EDCs to induce apoptosis, the modified IFP in the EDCs will be cleaved to activate the fluorescence signal. Flow-cytometry-based sorting of the IFP-positive EDCs and the following next-generation sequencing can identify the epitopes enriched in the sorted EDCs. Because the T-Scan method relies on the processing of the peptide library expressed in the EDCs, we applied the T-Scan method but with higher coverage of the proteome of SARS-CoV-2. We identified 70 high-confidence epitope peptides from four prevalent HLA-A subtypes in Han Chinese recovered COVID-19 patients. We validated several novel epitopes that are conserved across human coronaviruses, further supporting pre-existing cellular immunity. Importantly, we validated four epitope peptides that are mutated in the emerging variants of concern (VOCs), such as B.1.1.7 (Alpha variant), B.1.351 (Beta variant), P.1 (Gamma variant), and B.1.617.2 (Delta variant). We found evidence that these mutations led to decreased ability of the epitope to bind to the HLA complex. Our data provide evidence about how recently emerging SARS-CoV-2 variants evade cellular immunity, which might contribute to the increased transmissibility and pathogenicity of these variants.

RESULTS

T-Scan profiling reveals conserved CD8$^+$ T cell epitopes within the SARS-CoV-2 proteome

We designed the EDC library to cover the whole SARS-CoV-2 proteome with overlapping 56-amino-acid peptides in steps of one amino acid per peptide, totaling 9,179 peptides (Figure 1A). We generated four EDC libraries that express one of four highly

A

SARS-CoV2	V L L S V L Q Q L	S L E N V A F N V	L L L D D F V E I	L L D D F V E I I	T M A D L V Y A L
SARS-CoV	V L L S V L Q Q L	S L E N V A Y N V	L L L D D F V E I	L L D D F V E I I	T M A D L V Y A L
OC43	V L L N C L Q H L	S L E N V V Y N L	I L L D D F V T L	L L D D F V T L V	T M L D L C Y A L
HKU1	V L L N C L Q H L	S L E N V I Y N L	L L L D D F V V I	L L D D F V V I V	T M L D L C Y A L
NL63	V L L G C L S S M	S L E N I A F N V	L L L D D F V T I	L L D D F V T I L	T M M D L V Y A M
229E	V L M G I L S N M	G L E N I A F N V	L L L D D F V S V	L L D D F V S V L	T M M D L C F A L
Location	ORF1a	ORF1b	ORF1b	ORF1b	ORF1b
HLA genotype	A*02:01	A*02:01	A*02:01	A*02:01	A*02:01

SARS-CoV2	F C D L K G K Y V	H V E T F Y P K L	W L P T G T L L V	Y I C G F I Q Q K	S Q D L S V V S K
SARS-CoV	F C D L K G K Y V	H V E T F Y P K L	W L P T G T L L V	Y L C G F I K Q K	S Q D L S V I S K
OC43	L C K L R G K F V	K V M T F Y P R L	W L P A G T I L V	Y I C H M I R D K	S L N L N C V S K
HKU1	L C K L R G K F V	K I M T F Y P K M	W L P S G S I L V	Y I C Y L I R D K	S L N L N C V S K
NL63	Y C K F K G K C V	A V A T F Y P Q L	W L P P D A I I I	Y L N G V I R E K	S L D L G V I S K
229E	F C Q Y K G K W V	H L S T F Y P Q L	W L P H D A I V V	Y I N G F I C E K	S L D L T V V S K
Location	ORF1a	ORF1b	ORF1b	ORF1b	ORF1b
HLA genotype	A*02:07	A*02:07	A*02:07	A*11:01	A*11:01

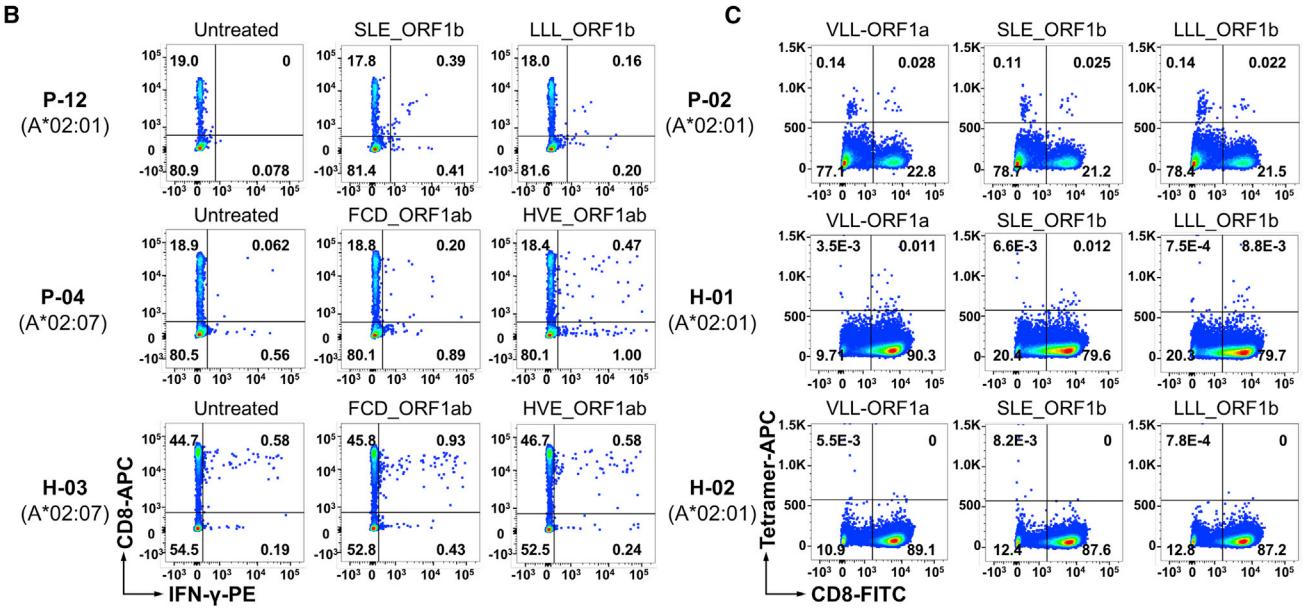

Figure 2. Validation of the identified CD8⁺ T cell epitopes conserved among human coronaviruses

(A) Alignment of the identified conserved CD8⁺ T cell epitopes among different coronavirus strains.

(B) IFN-γ intracellular cytokine staining (ICS) validation of conserved epitopes in COVID-19 convalescents (P-12) of the HLA-A*02:01 genotype, COVID-19 convalescents (P-04) of the HLA-A*02:07 genotype, and a healthy donor (H-03) of the HLA-A*02:07 genotype.

(C) MHC tetramer staining validation of three epitopes that are conserved among human coronaviruses in both COVID-19 convalescents (P-02) and 2 healthy donors (H-01 and H-02).

prevalent HLA-A subtypes (A*02:01, A*02:07, A*11:01, and A*24:02, which are expressed in 10.9%, 9.2%, 21.4%, and 14.4% of the Chinese population, respectively; Gonzalez-Galarza et al., 2020). HLA-genotyped CD8⁺ T cells were isolated from peripheral blood mononuclear cell (PBMC) samples of SARS-CoV-2 convalescents negative for both nucleic acid and SARS-CoV-2 antibody tests after infection. These samples (patients 1–8, 23, and 24) were taken at least 3 months after diagnosis (Table S1). The EDC library was incubated with CD8⁺ T cells with matching HLA-A subtype for 12 h and then the EDCs were sorted to enrich the IFP-positive population. The sorted cells were sequenced to quantitate the abundance of the epitopes expressed in the IFP-positive population. Further analysis takes advantage of the redundancy of epitopes embedded in the peptide library because the HLA-A epitope usually contains 9 or 10 amino acids. For example, most 9-mer epitopes are represented by 47 peptides in our library. To enrich high-confidence reoccurring epitopes, we required at least 8 peptides containing the same epitope to be enriched (Log2 > 2) to count as a hit epitope. We identified 70 high-confidence

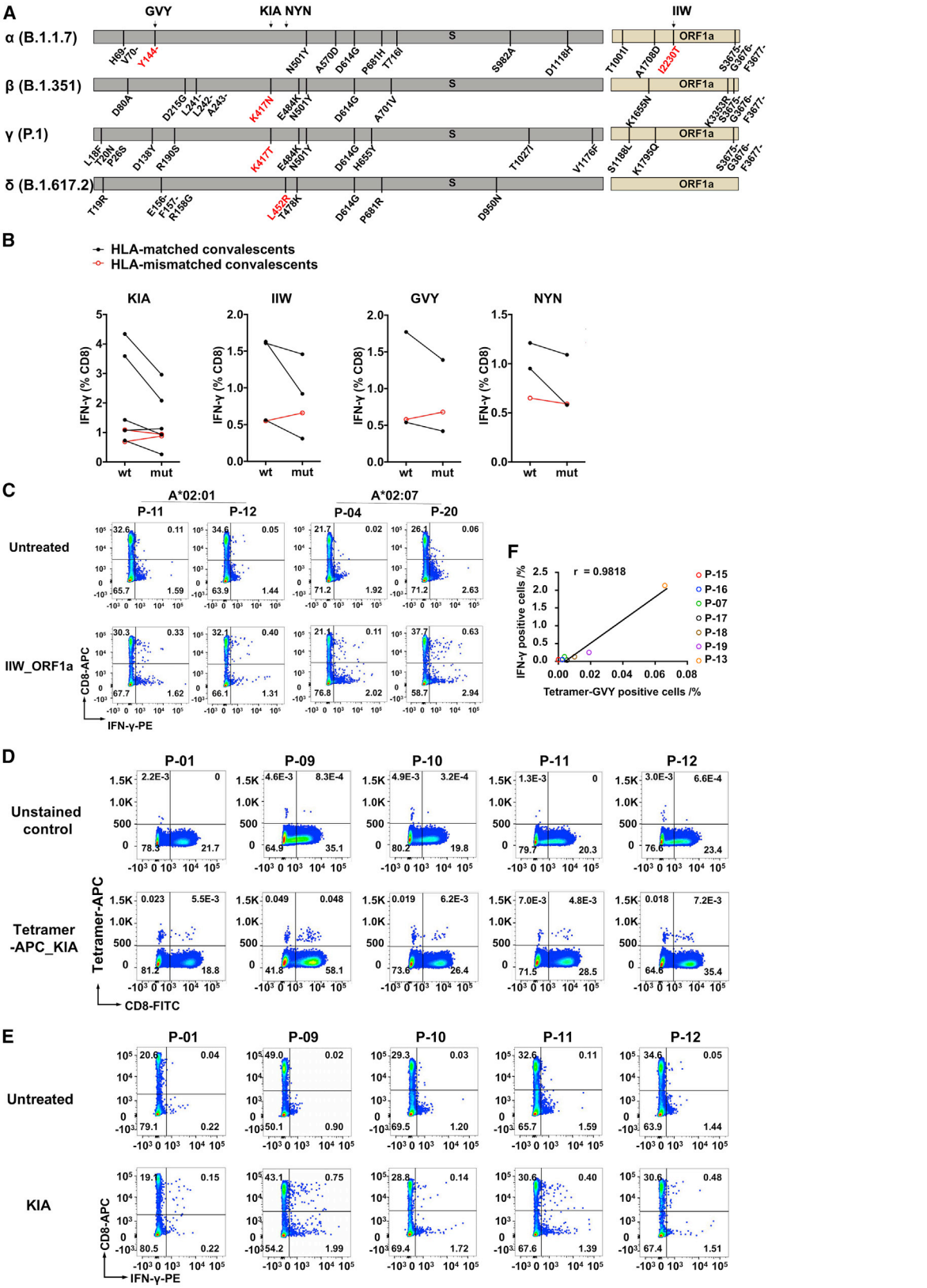

(legend on next page)

epitopes based on this threshold and the NetMHC 4.0 server prediction scores (strong binding scores based on the server), of which 20 have been identified in previous studies (Table S2). As shown in Figures 1B–1E, our T-Scan screening strongly enriched peptides in open reading frame 1a (ORF1a), ORF1b, and S. Among these 70 epitopes, we identified several that are conserved among the human coronaviruses (Figure 2A). We validated seven epitopes using synthetic peptides and showed that these peptides can activate $CD8^+$ T cells from convalescent and several healthy donors based on an interferon γ (IFN-γ) intracellular cytokine staining (ICS) assay (Figures 2B and S1; Table S3) (Schulien et al., 2021). We also generated the major histocompatibility complex (MHC) tetramer complex for three of the HLA-A*02:01 restricted epitopes and showed that they could stain not only a subpopulation of the $CD8^+$ T cells from a patient but one of two healthy donors tested (Figure 2C). Healthy donor H-01's $CD8^+$ T cells showed staining to all three MHC tetramers whereas those of healthy donor H-02 did not show staining. The results of these peptides, together with previously reported results (Braun et al., 2020; Grifoni et al., 2020; Habel et al., 2020; Le Bert et al., 2020; Mateus et al., 2020; Schulien et al., 2021; Tarke et al., 2021; Weiskopf et al., 2020), support the possibility of pre-existing cellular immunity in people not previously infected by SARS-CoV-2, which might contribute to different disease severity among people.

Validation of mutations in SARS-CoV-2 variants leading to reduced $CD8^+$ T cell responses in convalescent and vaccinated samples

Given the growing prevalence and concern of the SARS-CoV-2 variants, we focused on four epitopes identified in the profiling that are mutated in the B.1.1.7, B.1.351, P.1, or B.1.617.2 variants (Figure 3A). We first validated that these four epitopes can activate $CD8^+$ T cells in a majority of the SARS-CoV-2-vaccinated samples with matching HLA-A alleles based on IFN-γ staining (Figure S2) (CoronaVac; World Health Organization, 2021). Importantly, the variant-associated mutations in the four epitopes led to a significantly decreased activation of T cells from at least two convalescents (Figure 3B). Among them, IIW-ORF1a is predicted to bind both the HLA-A*02:01 and HLA-A*02:07 alleles, which was confirmed in two patient samples of each HLA-A allele (Figure 3C). Next, we generated recombinant tetramer complexes loaded with the cognate peptides of KIA_S and GVY_S. We show that KIA_S-MHC tetramers could stain a sub-population of patients with matching HLA-A alleles (Figure 3D), which was further validated by IFN-γ staining assay (Figure 3E). Importantly, the percentages of positive IFN-γ staining correlate with the percentages of tetramer staining (Figure 3F), supporting that these peptides are bona fide $CD8^+$ T cell epitopes. To test whether the variant-associated mutations escape the recognition of induced $CD8^+$ T cells by vaccination, we tested T cell samples from 33 vaccinated individuals 2–3 weeks post first-time immunization with the SARS-CoV-2 vaccine (CoronaVac) (World Health Organization, 2021), and found that the four epitope peptides activated T cells from a majority of the individuals in an HLA-subtype-specific manner (Figure 4; Table S4). Again, the variant-associated mutations in the four epitopes all led to a significantly decreased activation of T cells. These data suggest that SARS-CoV-2 variants evolved mutations that can evade T cell responses mediated by major HLA alleles.

Mechanism of immune evasion by mutations at K417, L452, and Y144 of the spike protein

To understand the molecular basis of the effect of the mutations on the epitope, we determined the crystal structure of HLA-A*02:01 in complex with the peptide epitope KIA_S at 2.8-Å resolution (Table S5). The structure revealed a strong binding between the two molecules. Analysis using the PDBePISA server (Krissinel, 2010; Krissinel and Henrick, 2007) counted 14 hydrogen bonds, 3 salt bridges, and 1 Pi-cation interaction between HLA and KIA_S (Figure 5A). At least 13 residues of HLA and 7 residues (all except for Y5 and Y7) of KIA_S are involved in the interactions. Importantly, the positively charged side-chain amino group of the N-terminal lysine (K1) of the KIA_S epitope adopts a Pi-cation interaction with the indole ring of W167 of HLA-A*02:01 (Figure 5B). The highly ordered electron density map of the closely positioned K1 of KIA_S and W167 of HLA suggests a strong interaction between the two (Figure 5B). Mutations of K1 to a chargeless asparagine (as in the B.1.351) or threonine (as in the P.1 variant) are expected to abolish this Pi-cation interaction at this position, consistent with the decreased binding scores predicted by the NetMHC 4.0 server (Figure 5C). We also determined the crystal structure of HLA-A*24:02 in complex with the peptide epitope NYN_S at 2.9-Å resolution (Figures 5D and 5E; Table S5). The structure illustrates a tight interaction between the two molecules that is supported by 18 hydrogen bonds and one salt bridge as calculated by the PDBePISA server. The hydrophobic side chain of L452 is buried in a pocket on the surface of HLA-A*24:02 (Figure 5E). Mutation of this leucine residue to a positively charged arginine as in the B.1.617.2 variant would disrupt this hydrophobic interaction and weaken the binding with HLA-A*24:02. For GVY_S, we performed structure-based docking simulations (Lee et al., 2015) using previously reported structural information of HLA (PDB:

Figure 3. Validation of the identified $CD8^+$ T cell epitopes containing mutation sites in recent circulating SARS-CoV-2 variants

(A) Representative mutation sites of four globally circulating SARS-CoV-2 variants.

(B) PBMCs from HLA-A*02:01 (KIA), HLA-A*02:07 (GVY), HLA-A*11:01 (GVY), or HLA*24:02 (NYN) -positive SARS-CoV-2 convalescents were expanded with the corresponding epitopes, and the frequency of IFN-γ-producing cells was measured by ICS.

(C) ICS validation of the IIW epitope in COVID-19 convalescents (P-11 and P-12) with the HLA-A*02:01 genotype and HLA-A*02:07 genotype (P-04 and P-20).

(D and E) Validation of the KIA epitope in 5 COVID-19 convalescents (P-01 and P-09 to P-12) with the HLA-A*02:01 genotype by both MHC tetramer staining and IFN-γ intracellular staining.

(F) The percentages of the ICS assay correlate positively with the percentages of the MHC tetramer staining assay. The correlation coefficient r was calculated using the Pearson correlation.

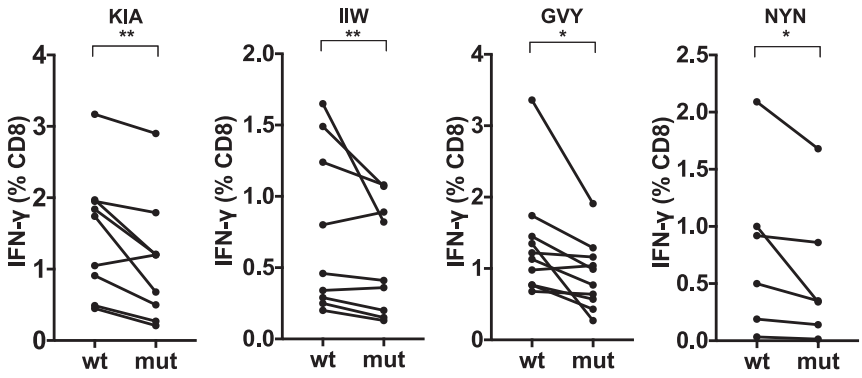

Figure 4. Mutations of SARS-CoV-2 variants decrease responses by CD8$^+$ T cells from vaccinated donors

PBMCs were isolated from HLA-A*02:01-, HLA-A*02:07-, HLA*11:01-, or HLA*24:02-positive donors who were vaccinated against SARS-CoV-2 2∼3 weeks post the first immunization (CoronaVac), and the frequency of IFN-γ-producing cells was measured by ICS, which reveals significantly decreased responses of CD8$^+$ cells after restimulation with mutant peptides compared to the corresponding wild-type peptides. Significance is indicated as *$p < 0.05$, **$p < 0.01$, tested by the Wilcoxon matched-pairs signed-rank test.

3mgo), which suggests weakened interaction between GVY_S and the HLA protein due to the deletion of Y144 in the B.1.1.7 variant (Figure S3). Moreover, we found that the mutations of KIA_S in the B.1.351 and P.1 variants (K417N/T) prevented the peptide from being loaded onto the recombinant HLA-A*02:01 molecules (Figure 5F), which is consistent with the predicted weaker binding scores of the mutant peptide compared to the canonical sequence (Figure 5C). Likewise, mutation of the GVY_S peptide in the B.1.1.7 variant hampered the formation of the tetramer complex, also consistent with the predicted scores (Figures 5C and 5G). Notably, mutations in both KIA_S and GVY_S are in the predicted anchoring sites of the epitopes, which are critical for epitope binding by the HLA protein (Oldstone, 1997). The L452R mutation did not prevent the formation of a complex with HLA-A*24:02 (Figure 5H), but the binding is likely formed through a different conformation of the epitope peptide with either reduced binding affinity or suboptimal recognition by the T cell receptor (TCR). Above all, we identified CD8$^+$ T cell epitopes that were mutated in three SARS-CoV-2 variants, suggesting the evasion of cellular immunity by these variants.

DISCUSSION

How emerging variant viruses rapidly become dominant is a burning question for understanding the dynamics of the epidemic and is critical for vaccine and therapy development (Challen et al., 2021; Davies et al., 2021b; Duffy et al., 2008; Sette and Crotty, 2021). Mounting evidence suggests these variants are resistant to currently available neutralizing antibodies generated against the original variant (Collier et al., 2021; Garcia-Beltran et al., 2021; Halfmann et al., 2020; Shen et al., 2021; Supasa et al., 2021; Wang et al., 2021a). However, these data cannot explain the highly increased transmissibility of the variants in mostly previously uninfected and unimmunized people. Furthermore, humoral immunity is not the only mechanism of host antiviral responses. Cellular immunity provides important host protection for reinfection (Kared et al., 2021; Nelde et al., 2021; Rha et al., 2021; Schulien et al., 2021). To date, mixed results have been reported regarding the infectivity of these variants (Davies et al., 2021a; Hou et al., 2020; Ozono et al., 2021; Volz et al., 2021; Yurkovetskiy et al., 2020; Zhou et al., 2021). A recent study has revealed that cellular immunity can be detected as early as 2–3 days from symptom onset and the strength of this early cellular immunity is strongly associated with mild disease and accelerated viral clearance (Le Bert et al., 2021; Tan et al., 2021). Another study has reported that mutations in the T cell epitopes of SARS-CoV-2 can help evade CD8 T cell response (Agerer et al., 2021). Because the binding of CD8$^+$ T cell epitopes to the HLA molecule requires the highly specific amino acid sequence of the epitope, evading cellular immunity provides an efficient way for the virus to gain advantages in replication and transmission. Here we provide evidence that evading cellular immunity might be a common characteristic of these dominating variants. We found four epitopes, three in the S protein and one in the nsp2 protein of ORF1a, to be mutated in the variants B.1.1.7, B.1.351, P.1, and B.1.617.2. Mutations in the KIA_S epitope occurred in more than one of the four variants. A previous study (Shomuradova et al., 2020) reported CD8$^+$ T cell reactivity to the KIA_S epitope in convalescent COVID-19 patients by MHC tetramer staining. This study examined the epitope specificity of the T cell immune response based on NetMHC 4.0 prediction results (Andreatta and Nielsen, 2016), and mainly reported two epitopes, YLQ_S and RLQ_S, that elicited CD8$^+$ T cell responses in most of the HLA-A*02:01 convalescents tested. KIA_S is in the list of verified epitopes that elicited CD8$^+$ T cell response in 6/17 convalescents. Besides KIA_S, YLQ_S is also a hit in our T-Scan screening (Table S2), which attests to the robustness of our screening. Analysis using recombinant HLA protein and structure analysis using X-ray crystallography and computational modeling all suggested a weakened interaction of the mutant peptides to HLA compared to the original epitopes KIA_S, NYN_S, and GVY_S. The K417N mutation of KIA_S is a particularly widespread mutation that cannot be explained by increasing infectivity or evading antibody neutralization (Greaney et al., 2021; Plante et al., 2021; Wang et al., 2021b). Our data support that this mutation might provide the advantage of evasion of cellular immunity. The L452R mutation has recently been reported to contribute to evasion from HLA-A24-mediated cellular immunity (Motozono et al., 2021), consistent with our findings. This mutation can also lead to increased viral infectivity, providing multiple benefits to the variants. Importantly, several VOCs harbor more than one mutation in the identified epitopes, providing a combinatorial effect to promote immune evasion covering multiple major HLA subtypes. In addition, our profiling has identified several epitopes that are highly conserved among human coronaviruses, particularly in ORF1a

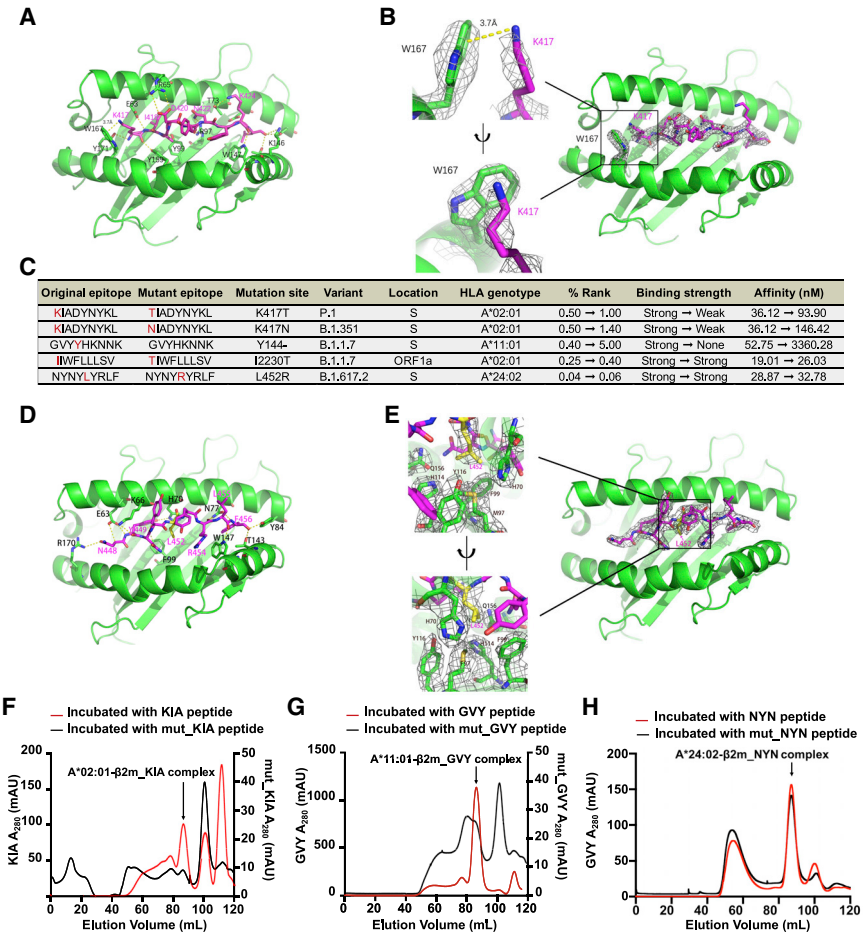

Original epitope	Mutant epitope	Mutation site	Variant	Location	HLA genotype	% Rank	Binding strength	Affinity (nM)
KIADYNYKL	TIADYNYKL	K417T	P.1	S	A*02:01	0.50 → 1.00	Strong → Weak	36.12 → 93.90
KIADYNYKL	NIADYNYKL	K417N	B.1.351	S	A*02:01	0.50 → 1.40	Strong → Weak	36.12 → 146.42
GVYYHKNNK	GVYHKNNK	Y144-	B.1.1.7	S	A*11:01	0.40 → 5.00	Strong → None	52.75 → 3360.28
IIWFLLLSV	TIWFLLLSV	I2230T	B.1.1.7	ORF1a	A*02:01	0.25 → 0.40	Strong → Strong	19.01 → 26.03
NYNYLYRLF	NYNYRYRLF	L452R	B.1.617.2	S	A*24:02	0.04 → 0.06	Strong → Strong	28.87 → 32.78

Figure 5. X-ray crystal structure of HLA-A*02:01 in complex with the KIA peptide and HLA-A*24:02 in complex with the NYN peptide

(A and B) Overview of the structure showing the interactions between HLA-A*02:01 and the KIA epitope (A) and an electron density map (2Fo − Fc map contoured at 1 σ) showing the electron density of the KIA_S epitope and W167 of HLA-A*02:01 (B).

(C) Summary of 4 identified epitopes from T-Scan profiling that contain the mutation site in recent circulating SARS-CoV-2 variants. % rank and the binding strength, as well as the affinity parameter, were predicted by NetMHC 4.0.

(D and E) Overview of the structure of HLA-A*24:02 and the NYN epitope (D) and the corresponding electron density map (E).

(F–H) Size-exclusion chromatography results of the purification of the A*02:01-β2m_peptide complex (F), A*11:01-β2m_peptide complex (G), and A*24:02-β2m_NYN complex (H) by incubating the β2 m and α chain with KIA/GVY/NYN peptides or the corresponding mutant peptides.

and ORF1b. These epitopes can support pre-existing immunity in people, partially explaining the differential disease severity among the population. Importantly, vaccines incorporating these epitope sequences might therefore elicit broad antiviral cellular responses.

Limitations of study

In this study, we demonstrated reduced CD8$^+$ T cell responses to synthetic peptides containing canonical or variant sequences using an ICS assay, which is a well-established surrogate assay commonly used by most studies on this subject (Motozono et al., 2021). Ideally, cells infected by bona fide canonical or variant viruses are to be used to test the T cell responses. However, we are limited by the access to bona fide variant viruses as well as access to a facility of sufficient biosafety containment. Nevertheless, our studies used a combination of biochemical, cellular, and structural data to provide strong evidence of reduced cellular responses of specific HLA-A subtypes to the epitope peptides containing the identified mutations in the variant viruses. Another potential limitation is that our experiments only measure a defined response of a particular HLA molecule to a short peptide of the virus. In real infections of humans, there are six alleles of HLA and hundreds of virus peptides involved, giving a much higher complexity. However, the four HLA subtypes we studied are four of the most frequent HLA subtypes. In addition, the multiple mutations we identified are within the same VOCs, providing a combinatorial effect. Importantly, previous studies of HIV mutations have demonstrated many examples of T cell epitope mutations associated with specific HLA subtypes being the driving force of HIV evolution dynamics at an individual or population level (Allen et al., 2005; Kawashima et al., 2009; Moore et al., 2002). These studies attest to the possibility of mutations in immunodominant epitopes leading to escape from cellular immune response.

STAR★METHODS

Detailed methods are provided in the online version of this paper and include the following:

- KEY RESOURCES TABLE
- RESOURCE AVAILABILITY
  - Lead contact
  - Materials availability
  - Data and code availability
- EXPERIMENTAL MODEL AND SUBJECT DETAILS
  - Cell lines
  - Primary cell cultures
  - E. coli cultures
- METHOD DETAILS
  - Isolation of peripheral blood mononuclear cells
  - Lentiviral production
  - SARS-CoV-2 library design and generation
  - SARS-CoV-2 T-Scan screen

- T cell expansion
- Intra-cytoplasmic cytokine staining (ICS)
- Preparation of pHLA tetramers
- MHC tetramer staining assay
- Molecular docking simulation of peptide-HLA-A2 complex

- QUANTIFICATION AND STATISTICAL ANALYSIS

SUPPLEMENTAL INFORMATION

Supplemental information can be found online at https://doi.org/10.1016/j.celrep.2021.109708.

ACKNOWLEDGMENTS

X.T. is supported by the China National Funds for Excellent Young Scientists (31722030) of the National Natural Science Fund and grants from the Beijing Advanced Innovation Center for Structural Biology, Beijing Frontier Research Center for Biological Structure, Tsinghua-Peking Center for Life Sciences, and the Spring Breeze Fund of Tsinghua University. T.J. is supported by the Strategic Priority Research Program of the Chinese Academy of Sciences (XDB29030104), National Natural Science Fund (grants 31870731 and 31971129), Fundamental Research Funds for the Central Universities (WK2070000108), and a COVID-19 special task grant supported by the Chinese Academy of Sciences Clinical Research Hospital (Hefei) (grant YD2070002017). This study was reviewed and approved by the Medical Ethical Committee of the First Affiliated Hospital of USTC (approvals 2020-XG(H)-014 and 2020-XG(H)-019). We thank the staff and patients of the First Affiliated Hospital of USTC and donors for their support in providing clinical samples. We also thank the staff at beamline 19U of the Shanghai Synchrotron Radiation Facility for their support during X-ray diffraction experiments. We thank Stephen Elledge, Xueqiang Zhao, and Xin Lin for reagents; Liuxin Tu for technical assistance; Yan Shi, Xiaohu Huang, Chen Dong, Huang Huang, and Deng Pan for discussion; and Bofeng Li for critical reading of the manuscript.

AUTHOR CONTRIBUTIONS

X.T. and T.J. conceptualized and supervised the study; H.Z. and L.R. performed T-Scan profiling and validation; S.D. and P.Z. performed protein purification and structure determination; X.H. assisted with clinical data collection; X.T. and T.J. wrote the manuscript with input from all authors.

DECLARATION OF INTERESTS

The authors declare no competing interests.

Received: May 14, 2021
Revised: July 28, 2021
Accepted: August 23, 2021
Published: September 14, 2021

REFERENCES

Agerer, B., Koblischke, M., Gudipati, V., Montaño-Gutierrez, L.F., Smyth, M., Popa, A., Genger, J.W., Endler, L., Florian, D.M., Mühlgrabner, V., et al. (2021). SARS-CoV-2 mutations in MHC-I-restricted epitopes evade CD8$^+$ T cell responses. Sci. Immunol. *6*, eabg6461.

Allen, T.M., Altfeld, M., Geer, S.C., Kalife, E.T., Moore, C., O'Sullivan, K.M., DeSouza, I., Feeney, M.E., Eldridge, R.L., Maier, E.L., et al. (2005). Selective escape from CD8$^+$ T-cell responses represents a major driving force of human immunodeficiency virus type 1 (HIV-1) sequence diversity and reveals constraints on HIV-1 evolution. J. Virol. *79*, 13239–13249.

Andreatta, M., and Nielsen, M. (2016). Gapped sequence alignment using artificial neural networks: application to the MHC class I system. Bioinformatics *32*, 511–517.

Braun, J., Loyal, L., Frentsch, M., Wendisch, D., Georg, P., Kurth, F., Hippenstiel, S., Dingeldey, M., Kruse, B., Fauchere, F., et al. (2020). SARS-CoV-2-reactive T cells in healthy donors and patients with COVID-19. Nature *587*, 270–274.

Calistri, P., Amato, L., Puglia, I., Cito, F., Di Giuseppe, A., Danzetta, M.L., Morelli, D., Di Domenico, M., Caporale, M., Scialabba, S., et al. (2021). Infection sustained by lineage B.1.1.7 of SARS-CoV-2 is characterised by longer persistence and higher viral RNA loads in nasopharyngeal swabs. Int. J. Infect. Dis. *105*, 753–755.

Campbell, F., Archer, B., Laurenson-Schafer, H., Jinnai, Y., Konings, F., Batra, N., Pavlin, B., Vandemaele, K., Van Kerkhove, M.D., Jombart, T., et al. (2021). Increased transmissibility and global spread of SARS-CoV-2 variants of concern as at June 2021. Euro Surveill. *26*, 2100509.

Cele, S., Gazy, I., Jackson, L., Hwa, S.H., Tegally, H., Lustig, G., Giandhari, J., Pillay, S., Wilkinson, E., Naidoo, Y., et al.; Network for Genomic Surveillance in South Africa; COMMIT-KZN Team (2021). Escape of SARS-CoV-2 501Y.V2 from neutralization by convalescent plasma. Nature *593*, 142–146.

Challen, R., Brooks-Pollock, E., Read, J.M., Dyson, L., Tsaneva-Atanasova, K., and Danon, L. (2021). Risk of mortality in patients infected with SARS-CoV-2 variant of concern 202012/1: matched cohort study. BMJ *372*, n579.

Chen, R.E., Zhang, X., Case, J.B., Winkler, E.S., Liu, Y., VanBlargan, L.A., Liu, J., Errico, J.M., Xie, X., Suryadevara, N., et al. (2021). Resistance of SARS-CoV-2 variants to neutralization by monoclonal and serum-derived polyclonal antibodies. Nat. Med. *27*, 717–726.

Collier, D.A., De Marco, A., Ferreira, I.A.T.M., Meng, B., Datir, R.P., Walls, A.C., Kemp, S.A., Bassi, J., Pinto, D., Silacci-Fregni, C., et al.; CITIID-NIHR BioResource COVID-19 Collaboration; COVID-19 Genomics UK (COG-UK) Consortium (2021). Sensitivity of SARS-CoV-2 B.1.1.7 to mRNA vaccine-elicited antibodies. Nature *593*, 136–141.

Davies, N.G., Abbott, S., Barnard, R.C., Jarvis, C.I., Kucharski, A.J., Munday, J.D., Pearson, C.A.B., Russell, T.W., Tully, D.C., Washburne, A.D., et al.; CMMID COVID-19 Working Group; COVID-19 Genomics UK (COG-UK) Consortium (2021a). Estimated transmissibility and impact of SARS-CoV-2 lineage B.1.1.7 in England. Science *372*, eabg3055.

Davies, N.G., Jarvis, C.I., Edmunds, W.J., Jewell, N.P., Diaz-Ordaz, K., and Keogh, R.H.; CMMID COVID-19 Working Group (2021b). Increased mortality in community-tested cases of SARS-CoV-2 lineage B.1.1.7. Nature *593*, 270–274.

Duffy, S., Shackelton, L.A., and Holmes, E.C. (2008). Rates of evolutionary change in viruses: patterns and determinants. Nat. Rev. Genet. *9*, 267–276.

Ferretti, A.P., Kula, T., Wang, Y., Nguyen, D.M.V., Weinheimer, A., Dunlap, G.S., Xu, Q., Nabilsi, N., Perullo, C.R., Cristofaro, A.W., et al. (2020). Unbiased screens show CD8$^+$ T cells of COVID-19 patients recognize shared epitopes in SARS-CoV-2 that largely reside outside the spike protein. Immunity *53*, 1095–1107.e3.

Garcia-Beltran, W.F., Lam, E.C., St Denis, K., Nitido, A.D., Garcia, Z.H., Hauser, B.M., Feldman, J., Pavlovic, M.N., Gregory, D.J., Poznansky, M.C., et al. (2021). Multiple SARS-CoV-2 variants escape neutralization by vaccine-induced humoral immunity. Cell *184*, 2372–2383.e9.

Gómez, C.E., Perdiguero, B., and Esteban, M. (2021). Emerging SARS-CoV-2 variants and impact in global vaccination programs against SARS-CoV-2/COVID-19. Vaccines (Basel) *9*, 243.

Gonzalez-Galarza, F.F., McCabe, A., Santos, E.J.M.D., Jones, J., Takeshita, L., Ortega-Rivera, N.D., Cid-Pavon, G.M.D., Ramsbottom, K., Ghattaoraya, G., Alfirevic, A., et al. (2020). Allele frequency net database (AFND) 2020 update: gold-standard data classification, open access genotype data and new query tools. Nucleic Acids Res. *48*, D783–D788.

Greaney, A.J., Loes, A.N., Crawford, K.H.D., Starr, T.N., Malone, K.D., Chu, H.Y., and Bloom, J.D. (2021). Comprehensive mapping of mutations in the

SARS-CoV-2 receptor-binding domain that affect recognition by polyclonal human plasma antibodies. Cell Host Microbe *29*, 463–476.e6.

Grifoni, A., Weiskopf, D., Ramirez, S.I., Mateus, J., Dan, J.M., Moderbacher, C.R., Rawlings, S.A., Sutherland, A., Premkumar, L., Jadi, R.S., et al. (2020). Targets of T cell responses to SARS-CoV-2 coronavirus in humans with COVID-19 disease and unexposed individuals. Cell *181*, 1489–1501.e15.

Habel, J.R., Nguyen, T.H.O., van de Sandt, C.E., Juno, J.A., Chaurasia, P., Wragg, K., Koutsakos, M., Hensen, L., Jia, X., Chua, B., et al. (2020). Suboptimal SARS-CoV-2-specific $CD8^+$ T cell response associated with the prominent HLA-A*02:01 phenotype. Proc. Natl. Acad. Sci. USA *117*, 24384–24391.

Halfmann, P.J., Hatta, M., Chiba, S., Maemura, T., Fan, S., Takeda, M., Kinoshita, N., Hattori, S.I., Sakai-Tagawa, Y., Iwatsuki-Horimoto, K., et al. (2020). Transmission of SARS-CoV-2 in domestic cats. N. Engl. J. Med. *383*, 592–594.

Hoffmann, M., Arora, P., Groß, R., Seidel, A., Hörnich, B.F., Hahn, A.S., Krüger, N., Graichen, L., Hofmann-Winkler, H., Kempf, A., et al. (2021). SARS-CoV-2 variants B.1.351 and P.1 escape from neutralizing antibodies. Cell *184*, 2384–2393.e12.

Hou, Y.J., Chiba, S., Halfmann, P., Ehre, C., Kuroda, M., Dinnon, K.H., III, Leist, S.R., Schäfer, A., Nakajima, N., Takahashi, K., et al. (2020). SARS-CoV-2 D614G variant exhibits efficient replication *ex vivo* and transmission *in vivo*. Science *370*, 1464–1468.

Kared, H., Redd, A.D., Bloch, E.M., Bonny, T.S., Sumatoh, H., Kairi, F., Carbajo, D., Abel, B., Newell, E.W., Bettinotti, M.P., et al. (2021). SARS-CoV-2-specific $CD8^+$ T cell responses in convalescent COVID-19 individuals. J. Clin. Invest. *131*, e145476.

Kawashima, Y., Pfafferott, K., Frater, J., Matthews, P., Payne, R., Addo, M., Gatanaga, H., Fujiwara, M., Hachiya, A., Koizumi, H., et al. (2009). Adaptation of HIV-1 to human leukocyte antigen class I. Nature *458*, 641–645.

Kechin, A., Boyarskikh, U., Kel, A., and Filipenko, M. (2017). cutPrimers: a new tool for accurate cutting of primers from reads of targeted next generation sequencing. J. Comput. Biol. *24*, 1138–1143.

Krissinel, E. (2010). Crystal contacts as nature's docking solutions. J. Comput. Chem. *31*, 133–143.

Krissinel, E., and Henrick, K. (2007). Inference of macromolecular assemblies from crystalline state. J. Mol. Biol. *372*, 774–797.

Kula, T., Dezfulian, M.H., Wang, C.I., Abdelfattah, N.S., Hartman, Z.C., Wucherpfennig, K.W., Lyerly, H.K., and Elledge, S.J. (2019). T-Scan: a genome-wide method for the systematic discovery of T cell epitopes. Cell *178*, 1016–1028.e13.

Le Bert, N., Tan, A.T., Kunasegaran, K., Tham, C.Y.L., Hafezi, M., Chia, A., Chng, M.H.Y., Lin, M., Tan, N., Linster, M., et al. (2020). SARS-CoV-2-specific T cell immunity in cases of COVID-19 and SARS, and uninfected controls. Nature *584*, 457–462.

Le Bert, N., Clapham, H.E., Tan, A.T., Chia, W.N., Tham, C.Y.L., Lim, J.M., Kunasegaran, K., Tan, L.W.L., Dutertre, C.A., Shankar, N., et al. (2021). Highly functional virus-specific cellular immune response in asymptomatic SARS-CoV-2 infection. J. Exp. Med. *218*, e20202617.

Lee, H., Heo, L., Lee, M.S., and Seok, C. (2015). GalaxyPepDock: a protein-peptide docking tool based on interaction similarity and energy optimization. Nucleic Acids Res. *43*, W431–W435.

Mateus, J., Grifoni, A., Tarke, A., Sidney, J., Ramirez, S.I., Dan, J.M., Burger, Z.C., Rawlings, S.A., Smith, D.M., Phillips, E., et al. (2020). Selective and cross-reactive SARS-CoV-2 T cell epitopes in unexposed humans. Science *370*, 89–94.

Moore, C.B., John, M., James, I.R., Christiansen, F.T., Witt, C.S., and Mallal, S.A. (2002). Evidence of HIV-1 adaptation to HLA-restricted immune responses at a population level. Science *296*, 1439–1443.

Motozono, C., Toyoda, M., Zahradnik, J., Saito, A., Nasser, H., Tan, T.S., Ngare, I., Kimura, I., Uriu, K., Kosugi, Y., et al.; Genotype to Phenotype Japan (G2P-Japan) Consortium (2021). SARS-CoV-2 spike L452R variant evades cellular immunity and increases infectivity. Cell Host Microbe *29*, 1124–1136.e11.

Mun, T., Chen, N.C., and Langmead, B. (2021). LevioSAM: fast lift-over of variant-aware reference alignments. Bioinformatics, btab396.

Neches, R.Y., Kyrpides, N.C., and Ouzounis, C.A. (2021). Atypical divergence of SARS-CoV-2 Orf8 from Orf7a within the coronavirus lineage suggests potential stealthy viral strategies in immune evasion. mBio *12*, e03014-20.

Nelde, A., Bilich, T., Heitmann, J.S., Maringer, Y., Salih, H.R., Roerden, M., Lübke, M., Bauer, J., Rieth, J., Wacker, M., et al. (2021). SARS-CoV-2-derived peptides define heterologous and COVID-19-induced T cell recognition. Nat. Immunol. *22*, 74–85.

Oldstone, M.B.A. (1997). How viruses escape from cytotoxic T lymphocytes: molecular parameters and players. Virology *234*, 179–185.

Ozono, S., Zhang, Y., Ode, H., Sano, K., Tan, T.S., Imai, K., Miyoshi, K., Kishigami, S., Ueno, T., Iwatani, Y., et al. (2021). SARS-CoV-2 D614G spike mutation increases entry efficiency with enhanced ACE2-binding affinity. Nat. Commun. *12*, 848.

Peng, Y., Mentzer, A.J., Liu, G., Yao, X., Yin, Z., Dong, D., Dejnirattisai, W., Rostron, T., Supasa, P., Liu, C., et al.; Oxford Immunology Network Covid-19 Response T Cell Consortium; ISARIC4C Investigators (2020). Broad and strong memory $CD4^+$ and $CD8^+$ T cells induced by SARS-CoV-2 in UK convalescent individuals following COVID-19. Nat. Immunol. *21*, 1336–1345.

Plante, J.A., Mitchell, B.M., Plante, K.S., Debbink, K., Weaver, S.C., and Menachery, V.D. (2021). The variant gambit: COVID-19's next move. Cell Host Microbe *29*, 508–515.

Rha, M.S., Jeong, H.W., Ko, J.H., Choi, S.J., Seo, I.H., Lee, J.S., Sa, M., Kim, A.R., Joo, E.J., Ahn, J.Y., et al. (2021). PD-1-expressing SARS-CoV-2-specific $CD8^+$ T cells are not exhausted, but functional in patients with COVID-19. Immunity *54*, 44–52.e3.

Sattler, A., Angermair, S., Stockmann, H., Heim, K.M., Khadzhynov, D., Treskatsch, S., Halleck, F., Kreis, M.E., and Kotsch, K. (2020). SARS-CoV-2-specific T cell responses and correlations with COVID-19 patient predisposition. J. Clin. Invest. *130*, 6477–6489.

Schulien, I., Kemming, J., Oberhardt, V., Wild, K., Seidel, L.M., Killmer, S., Sagar, Daul, F., Salvat Lago, M., Decker, A., et al. (2021). Characterization of pre-existing and induced SARS-CoV-2-specific $CD8^+$ T cells. Nat. Med. *27*, 78–85.

Sekine, T., Perez-Potti, A., Rivera-Ballesteros, O., Strålin, K., Gorin, J.B., Olsson, A., Llewellyn-Lacey, S., Kamal, H., Bogdanovic, G., Muschiol, S., et al.; Karolinska COVID-19 Study Group (2020). Robust T cell immunity in convalescent individuals with asymptomatic or mild COVID-19. Cell *183*, 158–168.e14.

Sette, A., and Crotty, S. (2021). Adaptive immunity to SARS-CoV-2 and COVID-19. Cell *184*, 861–880.

Shen, X., Tang, H., McDanal, C., Wagh, K., Fischer, W., Theiler, J., Yoon, H., Li, D., Haynes, B.F., Sanders, K.O., et al. (2021). SARS-CoV-2 variant B.1.1.7 is susceptible to neutralizing antibodies elicited by ancestral spike vaccines. Cell Host Microbe *29*, 529–539.e3.

Shomuradova, A.S., Vagida, M.S., Sheetikov, S.A., Zornikova, K.V., Kiryukhin, D., Titov, A., Peshkova, I.O., Khmelevskaya, A., Dianov, D.V., Malasheva, M., et al. (2020). SARS-CoV-2 epitopes are recognized by a public and diverse repertoire of human T cell receptors. Immunity *53*, 1245–1257.e5.

Supasa, P., Zhou, D., Dejnirattisai, W., Liu, C., Mentzer, A.J., Ginn, H.M., Zhao, Y., Duyvesteyn, H.M.E., Nutalai, R., Tuekprakhon, A., et al. (2021). Reduced neutralization of SARS-CoV-2 B.1.1.7 variant by convalescent and vaccine sera. Cell *184*, 2201–2211.e7.

Tan, A.T., Linster, M., Tan, C.W., Le Bert, N., Chia, W.N., Kunasegaran, K., Zhuang, Y., Tham, C.Y.L., Chia, A., Smith, G.J.D., et al. (2021). Early induction of functional SARS-CoV-2-specific T cells associates with rapid viral clearance and mild disease in COVID-19 patients. Cell Rep. *34*, 108728.

Tarke, A., Sidney, J., Kidd, C.K., Dan, J.M., Ramirez, S.I., Yu, E.D., Mateus, J., da Silva Antunes, R., Moore, E., Rubiro, P., et al. (2021). Comprehensive analysis of T cell immunodominance and immunoprevalence of SARS-CoV-2 epitopes in COVID-19 cases. Cell Rep. Med. *2*, 100204.

Trott, O., and Olson, A.J. (2010). AutoDock Vina: improving the speed and accuracy of docking with a new scoring function, efficient optimization, and multithreading. J. Comput. Chem. *31*, 455–461.

Volz, E., Hill, V., McCrone, J.T., Price, A., Jorgensen, D., O'Toole, Á., Southgate, J., Johnson, R., Jackson, B., Nascimento, F.F., et al.; COG-UK Consortium (2021). Evaluating the effects of SARS-CoV-2 spike mutation D614G on transmissibility and pathogenicity. Cell *184*, 64–75.e11.

Wang, P., Nair, M.S., Liu, L., Iketani, S., Luo, Y., Guo, Y., Wang, M., Yu, J., Zhang, B., Kwong, P.D., et al. (2021a). Antibody resistance of SARS-CoV-2 variants B.1.351 and B.1.1.7. Nature *593*, 130–135.

Wang, R., Zhang, Q., Ge, J., Ren, W., Zhang, R., Lan, J., Ju, B., Su, B., Yu, F., Chen, P., et al. (2021b). Analysis of SARS-CoV-2 variant mutations reveals neutralization escape mechanisms and the ability to use ACE2 receptors from additional species. Immunity *54*, 1611–1621.e5.

Weiskopf, D., Schmitz, K.S., Raadsen, M.P., Grifoni, A., Okba, N.M.A., Endeman, H., van den Akker, J.P.C., Molenkamp, R., Koopmans, M.P.G., van Gorp, E.C.M., et al. (2020). Phenotype and kinetics of SARS-CoV-2-specific T cells in COVID-19 patients with acute respiratory distress syndrome. Sci. Immunol. *5*, eabd2071.

World Health Organization (2021). WHO validates Sinovac COVID-19 vaccine for emergency use and issues interim policy recommendations. https://www.who.int/news/item/01-06-2021-who-validates-sinovac-covid-19-vaccine-for-emergency-use-and-issues-interim-policy-recommendations.

Yurkovetskiy, L., Wang, X., Pascal, K.E., Tomkins-Tinch, C., Nyalile, T.P., Wang, Y., Baum, A., Diehl, W.E., Dauphin, A., Carbone, C., et al. (2020). Structural and functional analysis of the D614G SARS-CoV-2 spike protein variant. Cell *183*, 739–751.e8.

Zhou, B., Thao, T.T.N., Hoffmann, D., Taddeo, A., Ebert, N., Labroussaa, F., Pohlmann, A., King, J., Steiner, S., Kelly, J.N., et al. (2021). SARS-CoV-2 spike D614G change enhances replication and transmission. Nature *592*, 122–127.

STAR★METHODS

KEY RESOURCES TABLE

REAGENT or RESOURCE	SOURCE	IDENTIFIER
Antibodies		
CD3 antibody (OKT3)	Thermo Fisher Scientific	Cat#306720
BV510 anti-human CD3	BioLengend	Cat#300448
PE anti-human IFN-γ	BioLengend	Cat#502509
FITC anti-human CD8	BD Biosciences	Cat#557085
Alexa 647 anti-human CD8	BD Biosciences	Cat#557708
Zombie NIR™ Fixable Viability Kit	BioLengend	Cat#423105
Bacterial and virus strains		
Stbl3 Chemically Competent Cell	Zomanbio	Cat#ZC108-1
Endura ElectroCompetent Cells (DUOS)	Lucigen	Cat#60242-1-LU
Chemicals, peptides, and recombinant proteins		
Interleukin-2, human (hIL-2)	Sigma (Millipore)	Cat#11147528001
Synthesized peptides	GenScript	N/A
MHC tetramer	This paper	N/A
Critical commercial assays		
GeneJET Genomic DNA Purification Kit	Thermo Fisher Scientific	Cat#K0722
Deposited data		
Crystallography data_HLA-A*02:01-KIA-S	https://www.rcsb.org	PDB code: 7EU2
Crystallography data_HLA-A*24:02-NYN-S	https://www.rcsb.org	PDB code: 7F4W
Experimental models: Cell lines		
HEK293T cells	ATCC	Cat#CRL-3216
HEK293T HLA-A*02:01 Epitope Discovery Cells (IFPGzB, ICARCR, HLA-A*02:01)	This paper	N/A
HEK293T HLA- A*02:07 Epitope Discovery Cells (IFPGzB, ICARCR, HLA-A*02:07)	This paper	N/A
HEK293T HLA- A*11:01 Epitope Discovery Cells (IFPGzB, ICARCR, HLA-A*11:01)	This paper	N/A
HEK293T HLA- A*24:02 Epitope Discovery Cells (IFPGzB, ICARCR, HLA-A*24:02)	This paper	N/A
Experimental models: Primary cell cultures		
PBMC	PBMC were isolated from human donors. The donor characteristics including age and gender are summarized in Tables S1, S3, and S4 PBMC collection was approved by the biomedical ethical committee of USTC.	N/A
Oligonucleotides		
Sequences listed in Table S6	N/A	N/A
Recombinant DNA		
SARS-CoV-2 peptidome library	This paper	N/A
pHAGE_EF1a_ICADCR_bsd	(Kula et al., 2019)	N/A
pHAGE_EF1a_IFPGzB_hyg	(Kula et al., 2019)	N/A
pHAGE_CMV_NFlageHA_DEST_IRES_puro	(Kula et al., 2019)	N/A
pHAGE_EF1a_HLA_A*02:01	Gift from Prof. Xin Lin's lab, Tsinghua University	N/A

(*Continued on next page*)

Continued

REAGENT or RESOURCE	SOURCE	IDENTIFIER
pHAGE_EF1a_HLA_A*02:07	Gift from Prof. Xin Lin's lab, Tsinghua University	N/A
pHAGE_EF1a_HLA_A*11:01	Gift from Prof. Xin Lin's lab, Tsinghua University	N/A
pHAGE_EF1a_HLA_A*24:02	Gift from Prof. Xin Lin's lab, Tsinghua University	N/A
Software and algorithms		
Bowtie	(Mun et al., 2021)	http://bowtie-bio.sourceforge.net/index.shtml
Cutadapt	(Kechin et al., 2017)	https://cutadapt.readthedocs.io/en/stable/

RESOURCE AVAILABILITY

Lead contact

Further information and requests for resources and reagents should be directed to and will be fulfilled by the Lead Contact, Xu Tan (xutan@tsinghua.edu.cn).

Materials availability

All unique/stable reagents generated in this study are indicated in the Key resources table and will be made available on request but may require a payment and/or a completed Materials Transfer Agreement if there is potential for commercial application.

Data and code availability

We have deposited the diffraction data as well as PDB of the crystallography data to the RCSB PDB: 7KEU, 7F4W.

This paper does not report original code.

Any additional information required to reanalyze the data reported in this work paper is available from the Lead Contact upon request.

EXPERIMENTAL MODEL AND SUBJECT DETAILS

Cell lines

HEK293T cells were cultured in DMEM (GIBCO, Cat # C11995500BT) with 10% (v/v) FBS, 100 units/mL penicillin (GIBCO, Cat # 15070063), and 0.1 mg/mL streptomycin (GIBCO, Cat # 15070063) at 37°C in 5% CO_2. The cells were authenticated by microscopic morphology examination and growth curve analysis and regularly checked by PCR tests to ensure to be free of mycoplasma.

Primary cell cultures

PBMC were isolated from human donors, including SARS-CoV-2 convalescents donors, healthy donors, as well as SARS-CoV-2 vaccinated donors, and the characteristics of PBMC donors are summarized in Tables S1, S3, and S4, respectively. Protocol of PBMC collection was approved by the biomedical ethical committee of USTC.

Isolated PBMC were cultured in RPMI (GIBCO, C11875500BT) with 10% (v/v) FBS, 100 units/mL penicillin, 0.1 mg/mL streptomycin, and 60U/ml IL-2 (Sigma, Cat # 11147528001) at 37°C in 5% CO_2.

E. coli cultures

All the *E.coli strains* used in this paper are cultured in 37°C with the shaking speed of 220rpm. The resistant gene of each plasmid is labeled in the end of the corresponding plasmid name which can be found in the Key resources table.

METHOD DETAILS

Isolation of peripheral blood mononuclear cells

The EDTA anticoagulant tubes were used to collect blood from recovered patients and normal people. All patients and healthy donors provided informed consents. Ficoll layering solution with a density of 1.077 was prepared using Ficoll 400 and Sodium diatrizoate to separate Peripheral Blood Mononuclear Cells (PBMCs). Gently add 3ml of whole blood to an equal volume of Ficoll layering solution in a 15ml conical tube at room temperature. Centrifuge at 400 g for 30 minutes at room temperature. During this step, the granulocytes, platelets and RBCs pellet to the bottom of the tube and the PBMCs float over the Ficoll layering solution. Carefully aspirate the cloudy-looking phase containing the PBMCs from the Ficoll-plasma interface. After washing the PBMCs with DMEM medium at

500 g at 4°C twice, 10 μl of cells were taken out and counted under a microscope. Finally, resuspend the cells with serum-free cell cryopreservation solution (Cat # C40100) and store in a −80°C refrigerator.

For expansion, 1 million PBMCs were seeded per well of a 24-well plate and stimulated with Dynabeads Human T-Activator CD3/CD28 (Thermo Fisher Scientific, Cat # 11161D) according to manufacturer's instructions.

$CD8^+$ memory T cells were isolated from the PMBC cells using the $CD8^+$ memory T cell isolation kit (Milenyi, Cat # 130-094-412) following the manufacturer's instructions. For expansion, $CD8^+$ memory T cells were cultured in RPMI-10% (v/v) FBS, 100 units/mL penicillin, 0.1 mg/mL streptomycin, 60U/ml IL-2 (Sigma, Cat # 11147528001), and 0.1 ug/ml anti-CD3 antibody (OKT3, Thermo Fisher Scientific, Cat # 306720).

Lentiviral production

Lentivirus was produced by transfecting HEK293T cells (ATCC, Cat # CRL-3216). For a 6-well cell plate, 1.5 μg lentiviral transfer vector, 1.5 μg pAX2 plasmid and 1 μg pMD2.G plasmid was co-transfected into HEK293T cells each well in a 6-well cell plate using the Neofect™ DNA transfection reagent (Cat # TF201201). Lentiviral supernatants were collected at 48h post-transfection and filtered through a 0.30 μm filter. For the cell line establishment, lentiviral supernatant was added to cells in the presence of 8 μg/ml polybrene.

SARS-CoV-2 library design and generation

To generate a complete set of potential SARS-CoV-2 antigens, we tiled across each ORF in 56 amino acids fragments with 55 amino acids overlap between adjacent tiles for a total of 9179 protein fragments. Fragment tiles were reverse translated using non-rare human codons. Each fragment was encoded by one nucleic acid sequence.

The oligo library was synthesized with the following adaptors according to the method of the previous published paper (Kula et al., 2019):

5′ adaptor: 5′ TGAATTCTGAGCTCG,
3′ adaptor: 5′ TCGGGTGCTCGAGCT.

The library was amplified with the following primers, containing overhangs encoding the BP recombination sites:

CMV_BP F: 5′ ggggacaagtttgtacaaaaaagcaggctcaGGAATTCTGAGCTCG
CMV_BP R: 5′ ggggaccactttgtacaagaaagctgggtcagctagttaAGCTCGAGCACCCGA

The amplified library was cloned into the pDONR221 vector using BP clonase (Thermo Fisher, Cat # 11789100) and then transfected into the pHAGE_CMV_NFlagHA_DEST_IRES_puro lentiviral vector using Gateway cloning (Thermo Fisher, Cat # 11791100). 150x library representation was maintained during all cloning steps. Plasmids were transfected to Endura ElectroCompetent Cells (Lucigen, Cat # 60242-1-LU) following the manuals.

The library was packaged into lentivirus and transduced at a representation of 1000 and MOI of 0.5 into HEK293T cells stably expressing pHAGE_EF1a_$ICAD^{CR}$, pHAGE_EF1a_ IFP^{GZB}, and pHAGE_EF1aHLA vector (HLA-A*02:01, HLA-A*02:07, HLA-A*11:01 and HLA-A*24:02 were overexpressed in HEK293T cells respectively). The cells were selected with 1 μg/ml puromycin for 3 days beginning 48h post-transduction. pHAGE_EF1a_$ICAD^{CR}$ plasmid and pHAGE_EF1a_ IFP^{GZB} plasmid were kindly offered by Prof. Stephen J. Elledge's lab (Harvard University). pHAGE_EF1a_HLA vectors (HLA-A*02:01, HLA-A*02:07, HLA-A*11:01 and HLA-A*24:02) were kindly offered by Prof. Xin Lin's lab (Tsinghua University). All the plasmids were transfected into Stbl3 Chemically Competent Cell for expansion (Zomanbio, Cat # ZC108-1).

SARS-CoV-2 T-Scan screen

For each HLA genotype, 20 million HEK293T cells (2100x library representation) expressing the SARS-CoV-2 library were co-cultured with 4 million HLA genotype-matched memory $CD8^+$ T cells of convalescent COVID-19 patients or healthy people for 12h, after which IFP^{GZB}-positive target cells were sorted by flow cytometry (BD, Influx). The genomic DNA of collected target cells were extracted by GeneJET Genomic DNA Purification Kit (Thermo Fisher Scientific, and Cat # K0722) for the preparation of deep-sequencing samples following the manuals (Novogene company). The sequencing data were analyzed by Bowtie (Mun et al., 2021) and Cutadapt (Kechin et al., 2017).

T cell expansion

PBMCs were thawed and pulsed with peptides (1 μg/ml) and cultured in RPMI-1640 (Cat # R0883) with 10% FBS, 10 mM HEPES (Sigma), 2 mM GlutaMAX (GIBCO), 50 IU/ml Pen-Strep (Sigma) and 50 IU IL-2 (Sigma, Cat # 11147528001) at a cell density of 1 million cells per ml. PBMCs were cultured for 10-12 days adding 100 IU IL-2 (Sigma, Cat # 11147528001) on day 5.

Intra-cytoplasmic cytokine staining (ICS)

About 0.2-1 million PBMCs were seeded per well in the 96-well cell plate with U-bottom. Add the candidate peptide (2 μg/ml) to the PBMCs and stimulate for 5h at 37°C in the presence of brefeldin A (BD, GlogiPlug, Cat # 555029; 0.5 μl/ml) and monensin (BD, GolgiStop, Cat # 554724; 0.325 μl/ml). Wash the cells by adding 150 μL PBS, centrifuge at 1000 g, 5 min, discard the supernatant

and stain cells with Zombie NIRTM Fixable Viability Kit (BioLegend, Cat # 423105) and antibodies of anti-CD3 (BioLegend, Brilliant Violet 510, Cat # 306720), anti-CD8 (BD PharMingen, Alexa Fluor 647, Cat # 557708) for 30min at 4°C. Then wash the cells with PBS twice, and add 100ul BD fixation/permeabilization solution (BD Cytofix/Cytoperm, Cat # 554714) per well for 20min at 4°C. Then wash the cells with 1x permeabilization buffer (BD Cytofix/Cytoperm, Cat # 554714), and stain cells with anti-IFN-γ (BioLegend, PE, Cat # 502509) for 15min at room temperature. Wash the cells with 1x permeabilization buffer twice and resuspend cells with PBS before analyzing by flow cytometry (BD LSRFortessa SORP). All the peptides were synthesized by the company of GenScript.

Preparation of pHLA tetramers

The sequence encoding biotin avidity protein (BAP: GLNDIFEAQKIEWH) was linked to the C terminus of the extracellular segment (residues 25-300) of class I HLA-A* α chain through a GS linker by PCR. The amplified PCR product was cloned into v1 vector under the control of T7 promoter with Sall and Not I restriction sites. The α chain was expressed in *E. coli* in the form of inclusion bodies, and the denatured α protein dissolved in 8 M urea was further purified by 6 × His using nickel affinity chromatography. At the same time, the recombinant protein β2 m-MBP (maltose binding protein) was expressed in *E. coli*, and the soluble β2 m protein was obtained by further digestion with TEV enzyme and further purification. For refolding, 3 mg of β2 m was added to 200 mL of cold refolding buffer (5 mM reduced L-Glutathione, 5 mM oxidized L-Glutathione, 2 mM EDTA, 5% glycerol, 1% sodium azide, 0.4 M $_L$-Arginine HCl, 0.1 M Tris-HCl, pH 8.0), and stir at 4°C for 2 h. Next, the mixture of 2 mg of peptide and 12 mg of α chain was dropped to the refolding buffer, and incubated at 4°C for 72 h. The refolded protein mixture was concentrated to a volume of 5 mL with a concentrator (membrane cutoff, 30 kDa), then purified by 120 mL of Superdex^{TM} 200 16/600 column (Cytiva HiLoad). The pHLA monomer part was eluted at approximately 80 mL of the 120 mL gel filtration. Biotinylated pHLA complex was obtained using BirA biotin kit (BirA-500, Avidity) and further purified by 24 mL of Superdex 200 10/30 column (GE Healthcare). Then biotinylated pHLA complex was coupled to APC-conjugated streptavidin to form a tetramer, which was used to stain PBMCs of COVID-19 patients.

MHC tetramer staining assay

Bulk PBMCs or isolated memory CD8$^+$ T cells were thawed, washed with warm RPMI-10%FBS media, and plated in U-bottom 96-well plates at 1 million cells/well. Cells were pelleted and resuspended with PBS with 1% FBS, as well as the corresponding tetramer at a final concentration of 10 μg per ml and incubated at 37°C for 15 min prior to adding the FITC-conjugated anti-human CD8 antibody (BD, Cat # 557085) and Zombie NIRTM Fixable Viability Kit (BioLegend, Cat # 423105), and incubating for an additional 15 min at room temperature. The stained cells were pelleted and washed three times before analyzed by flow cytometry (BD LSRFortessa SORP).

Molecular docking simulation of peptide-HLA-A2 complex

Molecular docking simulations of HLA-A2 were carried out with GalaxyPepdock for binding pattern evaluation. The available structure of HLAs: 0201 (PDB ID: 3mgo) and 1101(PDB ID: 1x7q) was downloaded from the RSCB PDB server (https://www.rcsb.org/) for modeling. GalaxyPepdock is a template-based docking program for peptides and proteins, which can generate 10 models to evaluate the results of the docking (Lee et al., 2015). The top model with the highest interaction similarity score was selected for next steps. The selected models were visualized by using Pymol 2.4 software. Autodock Vina 1.1 (Trott and Olson, 2010). was used for re-evaluation of binding affinity.

QUANTIFICATION AND STATISTICAL ANALYSIS

The data were analyzed using linear-regression analysis in Figure 3F (n = 7); Wilcoxon matched-pairs signed rank test in Figure 4 (For the test of KIA, IIW, GVY, NYN, n = 9, 9, 10, 6 respectively). In all figures, significance is indicated as *$p < 0.05$, **$p < 0.01$, ***$p < 0.001$, and the statistical data were presented as mean value. All statistical analyses were performed using GraphPad PRISM 8 software.